



## Compact Front-end Prototype for Next Generation RFI-rejecting Polarimetric L-band Radiometer

Jensen, Brian Sveistrup; Søbjærg, Sten Schmidl; Skou, Niels; Krozer, Viktor

*Published in:*  
Proceedings of the 39th European Microwave Conference

*Link to article, DOI:*  
[10.1109/EUMC.2009.5296530](https://doi.org/10.1109/EUMC.2009.5296530)

*Publication date:*  
2009

*Document Version*  
Publisher's PDF, also known as Version of record

[Link back to DTU Orbit](#)

*Citation (APA):*  
Jensen, B. S., Søbjærg, S. S., Skou, N., & Krozer, V. (2009). Compact Front-end Prototype for Next Generation RFI-rejecting Polarimetric L-band Radiometer. In Proceedings of the 39th European Microwave Conference IEEE. DOI: 10.1109/EUMC.2009.5296530

---

### General rights

Copyright and moral rights for the publications made accessible in the public portal are retained by the authors and/or other copyright owners and it is a condition of accessing publications that users recognise and abide by the legal requirements associated with these rights.

- Users may download and print one copy of any publication from the public portal for the purpose of private study or research.
- You may not further distribute the material or use it for any profit-making activity or commercial gain
- You may freely distribute the URL identifying the publication in the public portal

If you believe that this document breaches copyright please contact us providing details, and we will remove access to the work immediately and investigate your claim.

# Compact Front-end Prototype for Next Generation RFI-rejecting Polarimetric L-band Radiometer

Brian Sveistrup Jensen <sup>#1</sup>, Sten Schmidl Søjbjerg <sup>\*2</sup>, Niels Skou <sup>\*3</sup>, Viktor Krozer <sup>#4</sup>

<sup>#</sup>Department of Electrical Engineering - Microwave Technology Group, Technical University of Denmark

<sup>\*</sup>Danish National Space Institute, Technical University of Denmark

Ørsted's Plads, Building 348, DK-2800 Kgs. Lyngby, Denmark

<sup>1</sup>bsj@elektro.dtu.dk, <sup>2</sup>sss@space.dtu.dk

<sup>3</sup>ns@space.dtu.dk, <sup>4</sup>vk@elektro.dtu.dk

**Abstract**—Realizing the need for lower noise figure and smaller physical size in today's highly sensitive radiometers, this paper presents a new compact analog front-end (AFE) for use with the existing L-band (1400-1427 MHz) radiometer designed and operated by the Technical University of Denmark. Using sub-harmonic sampling to sample directly at the RF-frequency, this radiometer obtains a fully polarimetric response and enables detection and removal of radio frequency interference (RFI).

A more compact AFE will enable various desired features, as for example the ability to use the front-end with antenna arrays needing one receiver per antenna (Synthetic Aperture Radiometer, SARad), reduced weight for airborne missions and an easy temperature stabilization, i.e. improved instrument stability. The new front-end possesses an improved system noise temperature of only 76 K (roughly 40 K improvement) measured at an AFE physical temperature of 44°C, thus making the radiometer even more sensitive.

**Index Terms**—Microwave radiometry, Microwave receivers, Polarimetry, Calibration, Sub-harmonic sampling, Radio Frequency Interference.

## I. INTRODUCTION

Ocean salinity and soil moisture measurements by L-band radiometry, is presently an important issue as the European Space Agency (ESA) has scheduled to launch their soil moisture and ocean salinity (SMOS) mission in 2009. The payload of the mission satellite is the Microwave Imaging Radiometer using Aperture Synthesis (MIRAS) which is an L-band radiometer using a total of 69 antennas in a Y-shape to form a larger aperture. The Technical University of Denmark (DTU) has built a digital L-band radiometer for supporting ESA with calibration data - [1], [2]. This radiometer measures a fully polarimetric response, by feeding the received electrical signals, from a vertical and horizontal polarisation channel ( $E_V$  and  $E_H$  respectively) into a digital correlator circuit which outputs the full (brightness) Stokes vector given by

$$\overline{T}_B = \begin{bmatrix} I_B \\ Q_B \\ U_B \\ V_B \end{bmatrix} = \frac{\lambda^2}{k \cdot Z} \cdot \begin{bmatrix} \langle E_V^2 \rangle + \langle E_H^2 \rangle \\ \langle E_V^2 \rangle - \langle E_H^2 \rangle \\ 2 \cdot \Re \langle E_V \cdot E_H^* \rangle \\ 2 \cdot \Im \langle E_V \cdot E_H^* \rangle \end{bmatrix} \quad (1)$$

where  $\lambda$  is the wavelength,  $k$  is Boltzmann's constant ( $1.38 \cdot 10^{-23}$  [J·K<sup>-1</sup>]) and  $Z$  is the impedance of the medium in which the electric wave propagates. Here  $\langle \cdot \rangle$  denotes the

mean while  $\Re$  and  $\Im$  denotes the real and imaginary part, respectively.

The sampling is done by the radiometer digital front-end (DFE) directly at the RF-frequency, i.e. no down-conversion is performed, as is the case with many traditional radiometers such as the MIRAS. The DTU radiometer has been successfully flown on several missions around the world.

## II. SYSTEM REQUIREMENTS

The ocean salinity and soil moisture measurements demand a radiometer sensitivity (standard deviation),  $\Delta T$ , better than 0.1 Kelvin. Assuming constant gain over the integration time,  $\tau$ , and a flat passband spectrum over the bandwidth,  $B$ , the sensitivity is given by, [3],

$$\Delta T = C \cdot \frac{T_A + T_N}{\sqrt{B\tau}} \quad (2)$$

where  $T_A$  and  $T_N$  are the antenna brightness temperature and receiver noise temperature, respectively, and  $C$  is a constant that depends on the radiometer architecture. The new radiometer analog front-end (AFE) has been designed as a total power radiometer (TPR) where  $C = 1$ . For normal radiometry targets ( $0 < T_A < 300$  K) the old radiometer configuration obtains the 0.1 Kelvin sensitivity by use of a relatively low noise receiver ( $T_N \approx 115$  K) and an integration time of approximately 1 second. As the flight time between successive ground resolution cells is also approximately 1 second, [4], it might seem that a better receiver (less noisy) will not contribute in any appreciable way to the system performance. However, the radiometer DFE continuously search for abnormal measurements in order to reject radio frequency interference (RFI). This search is done in both time- and frequency- domain and any data not having a normal (Gaussian) distribution will be rejected. Doing this, the radiometer either lower the effective integration time or the effective bandwidth, thus degrading the radiometer sensitivity. Therefore, by lowering the receiver noise temperature,  $T_N$ , it is possible to reject samples while still obtaining a sensitivity,  $\Delta T$ , below 0.1 Kelvin.

For the normal instrument input power range of 0-300 Kelvin, the gain of the AFE should be approximately 85 dB, in order to provide the DFE with sufficient input power.

The above discussion and the simple fact that a smaller AFE will be easier to temperature stabilise and weigh less has been the motivation for the development of the new compact AFE. At the time of writing a new patch antenna system is under development. Compared to the presently used Potter horns, this will further reduce the total system size. Furthermore, it will become possible to use multiple AFE/antenna modules for synthesizing a much larger aperture, as done with the ESA-MIRAS instrument, thus obtaining better ground resolution.

### III. NEW COMPACT AFE

The existing AFE was built from a highly modular point of view using, for the most part of the design, of the shelf components (OTSC) interconnected with 50 Ohm cables. The approach used for the new AFE has been to design each of the radiometer functional blocks to meet the requirements and to fit a single enclosure without the use of interconnect cables.

The block diagram of the new AFE is shown in figure 1 and a photograph of the manufactured prototype is shown in figure 2. The radiometer consists of two identical receivers (vertical and horizontal polarization channels), each consisting of four modules - an LNA, an RF-amplifier, a main bandpass filter (BPF) and a Driver module that will amplify the signal to a proper level for the DFE which performs the sampling and computation of the four Stokes parameters. The RF-amplifier module serves only to get higher gain in front of the main bandpass filter and is not critical with respect to noise figure. Therefore the design of such is excluded from the following discussion.

In order to obtain correct measurements from the correlation channels, i.e. the third and fourth Stokes parameters,  $U_B$  and  $V_B$ , it is important that the two receivers have the same electrical length. In order to be able to calibrate differences between the two channels, the radiometer includes a noise injection network that, when turned on, will introduce an internal calibration point to the two receivers. The injected noise will be correlated (receiver-to-receiver), which means that it can be used for both amplitude- (gain curve extraction) and phase calibration (correlation channels). Specifically, the radiometer includes an automated calibration routine that will delay the sampling of one receiver as much as is required until a zero-reading is observed in the  $V_B$  channel.

The low-noise amplifier (LNA) has been of special interest to the design. Due to the inherent loss ( $\sim 0.2$  dB) of the 20 dB coupler located as the first component in each receiver, the LNA is required to possess a very low noise figure (NF). The LNA design is based on the brand new Ommic CGY2105XHV balanced LNA chip which, when used in a balanced amplifier configuration, obtains a noise figure of only 0.45 dB (including losses in  $90^\circ$  hybrids). The bandwidth of the LNA is approximately 3 GHz and because the noise figure has to be kept very low, no input filtering (besides that done by the antenna) is performed. Thus, high power sources RFI outside the protected L-band (1400-1427 MHz) has the potential for making the LNA saturate. Using a balanced LNA configuration with an LNA chip of high compression point,

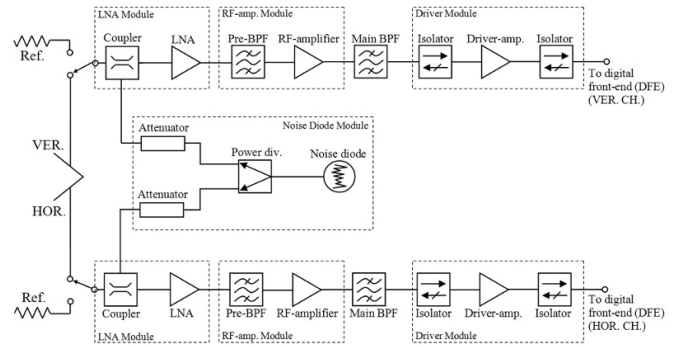


Fig. 1. Block diagram of the new compact AFE.

such as the CGY2105XHV, ensures a high dynamic range. Furthermore, it ensures a very high return loss on the input to the AFE, which is very important for radiometer applications.

The prototype main bandpass filter (BPF) is implemented as a stepped-impedance resonator bandpass filter (SIR-BPF) which selects the 27 MHz band of interest while subjecting the stopband to a 60 dB attenuation at  $\pm 50$  MHz. As the SIR-BPF consumes quite a lot of space, and as the design was to be compact, no such filter is put near the output of the AFE. Although the extra bandwidth of the Driver module ( $\sim 600$  MHz) will introduce more noise to the total output, this can be allowed if the gain distribution before and after the main filter is selected properly. For the new AFE a gain of 35 dB before and 50 dB after the main filter is selected. The future work on the AFE will seek to refine the design using the more compact surface acoustic wave (SAW) filters, still possible at L-band frequencies. This will enable an even further reduction in size.

As the signals of the two channels are to be correlated once they reach the DFE, it is very important that the isolation between the two channels is very good ( $>70$  dB, [4], [5]). If this is not the case, the leaked signal will eventually be correlated with itself, thus producing a high offset in the correlation channels ( $U_B$  and  $V_B$ ). One possible path where

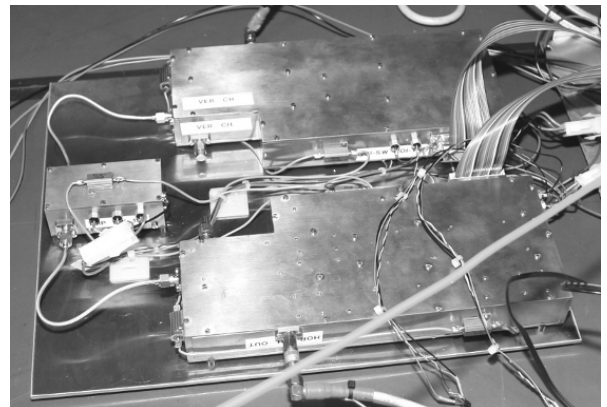


Fig. 2. Photo of the new compact AFE showing the two channels and the noise injection circuit in each of their enclosures.

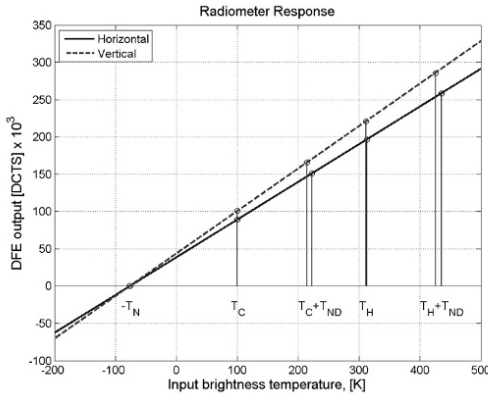


Fig. 3. Linearity test using two known well-matched loads with a brightness temperature of 77 K (cold,  $T_C$ ) and 310 K (hot,  $T_H$ ). The output units is digital counts (DCTS) which is a number generated from the DFE analog-to-digital conversion, detection and integration.

the signals can leak from one channel to the other, is the noise injection circuit. The desired isolation is obtained by the use of the 20 dB couplers, attenuators (also for lowering the amount of injected noise) and the high isolation inherently present in the lumped element Wilkinson power divider, used for splitting the signal from the noise diode equally between the channels. The estimated isolation is approximately 85 dB, and the measured results presented next verifies that no signals are leaking.

#### IV. MEASURED SYSTEM PERFORMANCE

The performance measurements done with the new AFE were focusing on three main purposes, each of which will be presented here. During the measurements the AFE was stabilized at a physical temperature of 44°C.

##### A. Receiver Noise Temperature, System Linearity & Noise Diode Calibration

The first step in verifying the design of the new AFE has been to conduct a linearity test. Here the receiver was subjected to two well-matched loads of known, and very different, brightness temperatures: *cold* load = 77 K and *hot* load = 310 K. Taking into account cable losses from the cryostat (the cold load) to the input of the AFE, the *cold* point becomes approximately 100 K. From this the system transfer function and noise temperature,  $T_N$ , can be derived as seen in figure 3 where the ordinate is in digital counts (DCTS) i.e. some number produced by the DFE analog-to-digital conversion. The test showed a noise temperature below 76 K for both channels.

By turning on the noise injection circuit, two extra inputs could be generated, i.e. *cold+noise* ( $T_C+T_{ND}$ ) and *hot+noise* ( $T_H+T_{ND}$ ). The first point is in a region where we strongly assume linearity, so this point can be used for calibration of the noise diode. Doing so, it is found that approximately 120 K of extra noise is injected into each channel. This enables a calibration of the system gain in the entire linear dynamic range of the analog-to-digital converter (ADC) located in the

DFE ( $\sim 10 - 500$  K referred to radiometer input, [4]). Using now the *hot+noise* point, the linearity of the system can be assessed. It is found, that the gain drops less than 1.5% when comparing the transfer curve between points  $T_C$  and  $T_C+T_{ND}$  to the transfer curve between points  $T_H$  and  $T_H+T_{ND}$ , and thus linearity is verified.

##### B. Sensitivity & Stability

From equation (2) it is seen that the worst sensitivity (highest  $\Delta T$ ) is obtained when the antenna input  $T_A$  is high. For the sensitivity and stability measurements it was therefore decided to have the radiometer receiver measure a hot well-matched load, approximately at room temperature. The instrument collected eight hours of data, and after having corrected the input noise temperature from the load, to take into account the variation in physical temperature, the sensitivity and stability were evaluated.

From the sensitivity formula, equation (2), we would expect that for an infinite integration time,  $\tau$ , the random white noise (with zero mean value), naturally present in the receiver, will cancel out and thus  $\Delta T$  should become infinitely small. However, real radiometer systems are not only affected by white noise, but also by flicker noise (1/f) and long-term drift, which means that at some point a longer integration time will not produce a better  $\Delta T$ . In fact, if  $\tau$  is further lengthened, at some point  $\Delta T$  will again start to rise due to the long-term drift.

The standard deviation,  $\sigma_y$ , of any data set,  $y(n)$ , can be found by taking the square root of the variance,  $\sigma_y^2$ , of that data set. It has been shown that the normal variance, i.e. the one found by looking at the entire data set at once, will not converge for the flicker noise and long-term drift contributions to the system noise, and thus do not predict the correct sensitivity. Instead, using the so-called Allan variance also called the two-sample variance, given by, [6]

$$\sigma_y^2 = \frac{1}{2} \langle (y_{n+1} - y_n)^2 \rangle \quad (3)$$

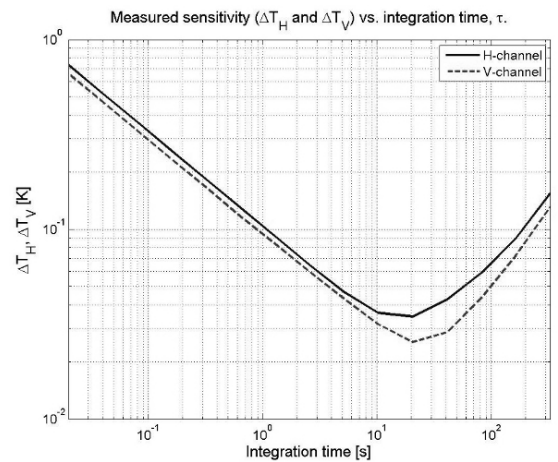


Fig. 4. Sensitivity and stability test of the new AFE using 8 hours of measured data of a hot (room temperature) termination.

all noise contributions will be taken into account.

Figure 4 shows the measured result. Just as expected, we see that for the first part of the curves, white noise is the dominant noise contributor in that the  $(1/\sqrt{\tau})$  term of the sensitivity formula, equation (2), produces a straight line with a negative slope in the log-scale plot. Then at an integration time of approximately 10 seconds the curves break and flatten out. This is where the flicker noise begins to dominate the performance. Then at approximately 40 seconds integration time the long-term drift makes the curves start rising again. To obtain a sensitivity below 0.1 K an integration time of approximately 1 second should be used and it is seen that the instrument is stable within approximately 200 seconds. This relatively poor sensitivity is mainly due to inadequate temperature stabilization as discussed next.

During the experiments the existing temperature stabilizing circuit was used. One problem arose from this scheme. As the new AFE did not fit the existing instrument case, no air exchange control could be utilised, thus leaving only heating (by use of power resistors) as an option. Looking at the output frequency spectrum of various temperature sensors located within the new AFE, showed that a distinct frequency component was located at around 0.054 Hz (time period of 18.5 seconds), thus indicating that the temperature regulating circuit (and thereby the instrument physical temperature) was oscillating. As seen from figure 4 this coincides well with the point where the sensitivity is at its minimum, i.e. where drift starts to become the dominant noise contributor. It is therefore believed that the instrument can be made much more stable (even more stable than the old one:  $\sim 15$  minutes) once a proper temperature regulating scheme is implemented.

### C. Channel Isolation & Delay Alignment

Figure 5 shows the raw output of the  $U_B$  and  $V_B$  channels when the noise diode is switched off and when it is switched on. The data set is the same as above with an integration time of 1 second. When the noise diode is switched off we see that the correlation channels stay within  $\pm 0.5$  Kelvin of the expected value (zero). This is satisfactory as the DFE itself is expected to produce a small offset and can be corrected for in the calibration. Thus, it is concluded that a very high isolation is established between the horizontal and vertical channels.

When the noise diode is switched on, we would expect to see twice the amount of noise diode input noise temperature, i.e. approximately 240 Kelvin, in the  $U_B$ -channel and 0 K in the  $V_B$ -channel. However, from the plots we see that the  $U_B$ -channel shows a 196 Kelvin reading while the  $V_B$ -channel shows a 64 Kelvin reading. As the  $V_B$ -channel is not zero it is concluded that the channels are not electrically aligned and thus some phase adjustment is needed during a full calibration of the radiometer. The DFE includes a special routine for this calibration step, called "delay alignment", which will automatically skew the sampling of one channel compared to the other until a zero-reading is obtained in  $V_B$ .

From the two receiver outputs we find that the total power that enters into the correlation channels is  $\sqrt{196^2 + 64^2} =$

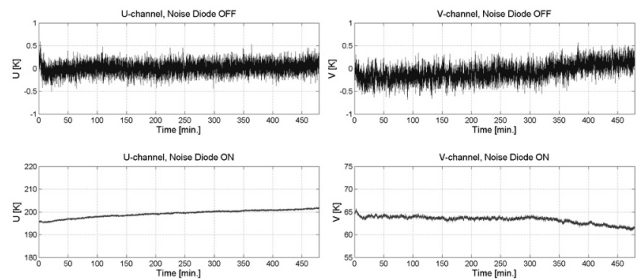


Fig. 5. Channel isolation test showing results when the noise injection circuit is turned off and on.

206.2 Kelvin, i.e. approximately 35 Kelvin below the expected value. This is a direct consequence of a small frequency misalignment between the main filters of the horizontal and vertical channels and will have to be taken into account during calibration.

## V. CONCLUSIONS

A new compact AFE prototype, one fourth the size of the old AFE, has been developed for use with the fully polarimetric L-band radiometer, operated by the Technical University of Denmark. It is estimated that a refined version of the prototype will be approximately half the size of the presented design.

The new AFE has an improved noise temperature of only 76 K (measured at an AFE physical temperature of 44°C), thus enabling higher sensitivity. For use in RFI-rejection techniques it is now possible to reject samples in time or frequency while still obtaining the desired sensitivity of 0.1 K. Experience from previous instrument designs show that the new AFE, as it was measured with a poor temperature stabilisation, possesses good stability. Thus, for improving the instrument stability a better temperature stabilising control mechanism is needed. Future missions will serve to validate the improvements to the RFI-rejecting techniques now possible.

## REFERENCES

- [1] N. Skou, S. S. Søjbjerg, J. E. Balling, and S. S. Kristensen, "A second generation L-band digital radiometer for sea salinity campaigns," in *Proceedings of IGARSS'06*. Technical University of Denmark, 2006, Presented at: IGARSS'06, 2006.
- [2] J. Rotboll, S. S. Søjbjerg, and N. Skou, "A novel L-band polarimetric radiometer featuring subharmonic sampling," *Radio Science*, vol. 38, no. 3, pp. –, March 2003.
- [3] F. T. Ulaby, R. K. Moore, and A. K. Fung, *Microwave Remote Sensing*. Massachusetts 01867, USA: Addison-Wesley Publishing Company, Inc., 1981, vol. 1 (Active and Passive), ISBN: 0-201-10759-7.
- [4] S. S. Søjbjerg, "Polarimetric Radiometers and their Applications," Ph.D. dissertation, Electromagnetic Systems, Ørsted-DTU, Technical University of Denmark (DTU), November 2002.
- [5] B. S. Jensen, "Compact Front-end for L-band Radiometer," Master's thesis, National Space Institute - Technical University of Denmark (DTU), September 2008.
- [6] G. Rau, R. Schieder, and B. Vowinkel, "Characterization and measurement of radiometer stability," in *Proc. 14th European Microwave Conference*, Oct. 1984, pp. 248–253.